Stem Cell Reports
Article
ISSCR
OPEN ACCESS

Sox2-Mediated Conversion of NG2 Glia into Induced Neurons in the Injured Adult Cerebral Cortex

Christophe Heinrich,[1,2,7] Matteo Bergami,[1,7,9] Sergio Gascón,[1,3] Alexandra Lepier,[1] Francesca Viganò,[1] Leda Dimou,[1,3] Bernd Sutor,[1] Benedikt Berninger,[1,4,5,8,*] and Magdalena Götz[1,3,6,8,*]

[1]Physiological Genomics, Institute of Physiology, Ludwig-Maximilians University Munich, 80336 Munich, Germany
[2]INSERM U836, University Grenoble Alpes, Grenoble Institute of Neurosciences, 38000 Grenoble, France
[3]Institute for Stem Cell Research, National Research Center for Environment and Health, 85764 Neuherberg, Germany
[4]Institute of Physiological Chemistry, University Medical Center, Johannes Gutenberg University Mainz, 55128 Mainz, Germany
[5]Focus Program Translational Neuroscience, Johannes Gutenberg University Mainz, 55131 Mainz, Germany
[6]Munich Cluster for Systems Neurology (SyNergy), 80336 Munich, Germany
[7]Co-first author
[8]Co-senior author
[9]Present address: Cologne Excellence Cluster on Cellular Stress Responses in Aging-Associated Diseases (CECAD), University Hospital, 50931 Köln, Germany
*Correspondence: berningb@uni-mainz.de (B.B.), magdalena.goetz@helmholtz-muenchen.de (M.G.)
http://dx.doi.org/10.1016/j.stemcr.2014.10.007

SUMMARY

The adult cerebral cortex lacks the capacity to replace degenerated neurons following traumatic injury. Conversion of nonneuronal cells into induced neurons has been proposed as an innovative strategy toward brain repair. Here, we show that retrovirus-mediated expression of the transcription factors *Sox2* and *Ascl1*, but strikingly also *Sox2* alone, can induce the conversion of genetically fate-mapped NG2 glia into induced doublecortin $(DCX)^+$ neurons in the adult mouse cerebral cortex following stab wound injury in vivo. In contrast, lentiviral expression of *Sox2* in the unlesioned cortex failed to convert oligodendroglial and astroglial cells into DCX^+ cells. Neurons induced following injury mature morphologically and some acquire NeuN while losing DCX. Patch-clamp recording of slices containing *Sox2*- and/or *Ascl1*-transduced cells revealed that a substantial fraction of these cells receive synaptic inputs from neurons neighboring the injury site. Thus, NG2 glia represent a potential target for reprogramming strategies toward cortical repair.

INTRODUCTION

In the adult forebrain, neurogenesis is restricted to few neurogenic regions such as the subependymal zone of the lateral ventricle and the subgranular zone of the dentate gyrus (Gage and Temple, 2013). In contrast, the adult cerebral cortex is devoid of on-going neurogenesis and traumatic injury does not elicit a neurogenic regenerative response but rather creates a gliogenic environment (Buffo et al., 2005; Robel et al., 2011). Previous work in vitro showed that different types of somatic cells, including astroglia and pericytes of brain origin, can be directly converted into functional neuronal cells by forced expression of key neurogenic transcription factors (Arlotta and Berninger, 2014). For instance, we and others demonstrated that astroglia and oligodendrocyte progenitor cells (OPCs) isolated from the postnatal mouse cerebral cortex can be directed toward a neuronal identity by forced expression of the transcription factors *Pax6*, *Neurog2*, *Ascl1*, *NeuroD1*, or *Pou3f4* and *Sox11* (Berninger et al., 2007; Guo et al., 2014; Heinrich et al., 2010; Heins et al., 2002; Ninkovic et al., 2013) and that astroglia-to-neuron conversion is facilitated by high levels of *Sox2* expression (Heinrich et al., 2010). We also showed that cells of pericytic origin isolated from the adult human cerebral cortex can be reprogrammed into functional neurons by combined expression of *Sox2* and *Ascl1* (Karow et al., 2012). Moreover, combined expression of *Ascl1*, *Brn2*, and *Myt1l* mediated conversion of adult mouse parenchymal striatal astrocytes into induced neurons in vivo (Torper et al., 2013), whereas *Sox2* was sufficient to reprogram mouse striatal or spinal cord astrocytes into neuroblasts (Niu et al., 2013; Su et al., 2014). However, it has been difficult to induce neurons after invasive brain injury, such as stab wound or stroke, especially in the injured cerebral cortex (Buffo et al., 2005; Grande et al., 2013). This need for improved reprogramming after invasive injury conditions prompted us to test in vivo whether the combination of *Sox2* and *Ascl1* would allow for generating induced neurons after traumatic injury in the adult mouse cerebral cortex.

RESULTS

Nonneuronal Cells Proliferating after Cortical Injury Are Converted into Doublecortin$^+$ Cells upon Forced Coexpression of *Sox2* and *Ascl1*

In this study, we aimed at converting reactive glial cells into induced neurons in the adult cerebral cortex in the context of acute invasive injury. We used a mouse model of traumatic injury induced by a local stab wound inflicted to the upper layers of the cerebral cortex (Bardehle et al.,

2013; Buffo et al., 2005). This resulted in severe reactive gliosis characterized at 7 days postlesion by astrogliosis as revealed by GFAP upregulation and reactive astrocyte hypertrophy (Figures S1A and S1A′ available online), activation of microglia (Figures S1B and S1B′), and proliferation of NG2 glia as previously described (Dimou and Götz, 2014). To investigate whether proliferative nonneuronal cells reacting to injury can be reprogrammed into induced neurons during on-going reactive gliosis, we used a retrovirus strategy to deliver neurogenic transcription factors into the injured tissue at 3 days postlesion (Figure 1A). The rationale for using retroviral vectors was to exclusively target nonneuronal cells that actively proliferate in response to injury, thereby excluding neurons but also nonproliferative glia from transduction as previously reported (Buffo et al., 2005). Injection of a Moloney-murine-leukemia-virus-based control retrovirus (pCAG-IRES-*Dsred*) resulted in labeling of high numbers of proliferative glial populations throughout all cortical layers 10–12 days postinjection (dpi; Figure 1B). Whereas most labeled cells were NG2 glia immunoreactive for NG2 and OLIG2 (59.3% ± 4.4% of DSRED$^+$ cells at 10.3 ± 0.3 dpi; n = 3 mice; Figures S1C–S1D″), the remainder of the DSRED$^+$ cells were either GFAP$^+$ reactive astrocytes (Figures S1E–S1E″) or IBA1/CD45$^+$ microglia (Figures S1F–S1F″). Importantly, in control retrovirus-injected mice, none of the transduced but also none of the untransduced cells expressed the immature neuronal marker doublecortin (DCX) (Figures 1C and 1I; 1,711 DSRED$^+$ cells counted at 10.3 ± 0.3 dpi; n = 3 mice), confirming the lack of endogenous cortical neurogenesis after stab wound injury including in layer I, in contrast to the spontaneous neurogenesis reported after ischemia (Ohira et al., 2010). Furthermore, we did not observe migration of DCX$^+$ cells from the white matter or adult neurogenic zones (Figure 1C), due to the highly localized injury restricted to the upper layers of the gray matter.

To reprogram these reactive glial cells into neurons, we injected a retrovirus encoding the transcription factor *Ascl1* (pCAG-*Ascl1*-IRES-*Dsred*) 3 days after stab-wound injury. Surprisingly, despite high numbers of DSRED$^+$ cells, very few expressed DCX (1.0% ± 0.5%; 1,330 DSRED$^+$ cells counted; 11 dpi; n = 3 mice; Figures 1D–1F and 1I). Based on our previous data showing synergy between *Sox2* and *Ascl1* for inducing neuronal reprogramming (Karow et al., 2012), we coinjected two retroviruses encoding *Sox2* (pCAG-*Sox2*-IRES-*Gfp*) and *Ascl1* (pCAG-*Ascl1*-IRES-*Dsred*). Many proliferating cells in the lesion area were cotransduced by both retroviruses (29.7% ± 15.0% of the transduced cells; Figures 1G and 1J). In contrast to the lack of *Ascl1*-induced neurogenesis, forced expression of *Sox2* and *Ascl1* elicited appearance of DCX$^+$ cells located close to the injection site within the injured cortical area (Figures 1G and 1H) and representing approximately one-third of the double-transduced cells at ~12 dpi (30.2% ± 2.6% at 12.7 ± 2.7 dpi; 686 double-transduced cells counted; n = 3 mice; Figure 1I). Many of these exhibited an immature neuronal morphology, extending relatively long and branched processes (Figures 1J–1L and S2A–S2F). Closer to the lesion center, more neurons were induced than in more peripheral areas (Figures 1G, 1H, and S2C). Consistent with restriction of retroviral transduction to cells undergoing cell division, the newly emerging DCX$^+$ cells incorporated the thymidine-analog bromodeoxyuridine (BrdU) given for 10 consecutive days after viral injection (Figures S2G–S2G″). Taken together, our data demonstrate that *Sox2* and *Ascl1* induce conversion of nonneuronal cells into DCX$^+$ neurons in the injured adult murine cortex.

Nonneuronal Cells Proliferating after Cortical Injury Are Converted into Induced Neurons upon Forced Expression of *Sox2* Alone

Notably, we also encountered DCX$^+$ cells that appeared to be only transduced by the virus encoding *Sox2* (Figures 1M–1O). About 20% of these GFP$^+$ (i.e., *Sox2*) only cells were DCX$^+$ (21.8% ± 10.2%; 490 GFP$^+$ cells counted; n = 3 mice; Figure S2H), indicating that *Sox2* alone may be sufficient to induce neuronal conversion of injury-responsive cells. In contrast, very few DSRED$^+$ cells expressing *Ascl1* only were converted into DCX$^+$ cells, confirming our previous observations on the very limited neuronal conversion induced by *Ascl1* (1.2% ± 0.6%; 510 DSRED$^+$ cells counted; n = 3 mice; Figure S2H).

To exclude low levels of *Ascl1* coexpression in *Sox2*-induced neurons below detection provided by the DSRED reporter, we injected the *Sox2*-encoding retrovirus alone into the stab-wound-lesioned cortex (pCAG-*Sox2*-IRES-*Gfp*). In all mice, we found that a substantial number of *Sox2*-transduced cells had differentiated into DCX$^+$ cells exhibiting a neuronal morphology at ~12 dpi (13.9% ± 3.5% at 12.3 ± 1.6 dpi; 2,057 GFP$^+$ cells counted; n = 4 mice; Figures 2A, 2B, and 1I), confirming that *Sox2* alone can induce neuronal conversion of nonneuronal cells, although to a lower extent compared to combined expression of *Sox2* and *Ascl1*. Strikingly, however, in *Sox2*-virus-injected mice, occasionally large clusters of densely packed transduced DCX$^+$ cells could be observed along the lesion track (Figures 2C and 2D; Movie S1). As these densely packed clusters of DCX$^+$ cells could not be quantified, our quantifications of induced neurons are likely an underestimation. To assess whether retrovirus-driven *Sox2* expression was maintained for several days after virus delivery, we performed immunohistochemistry for GFP, SOX2, and DCX at 12 dpi. All GFP-transduced cells were immunoreactive for SOX2, although with some variability in

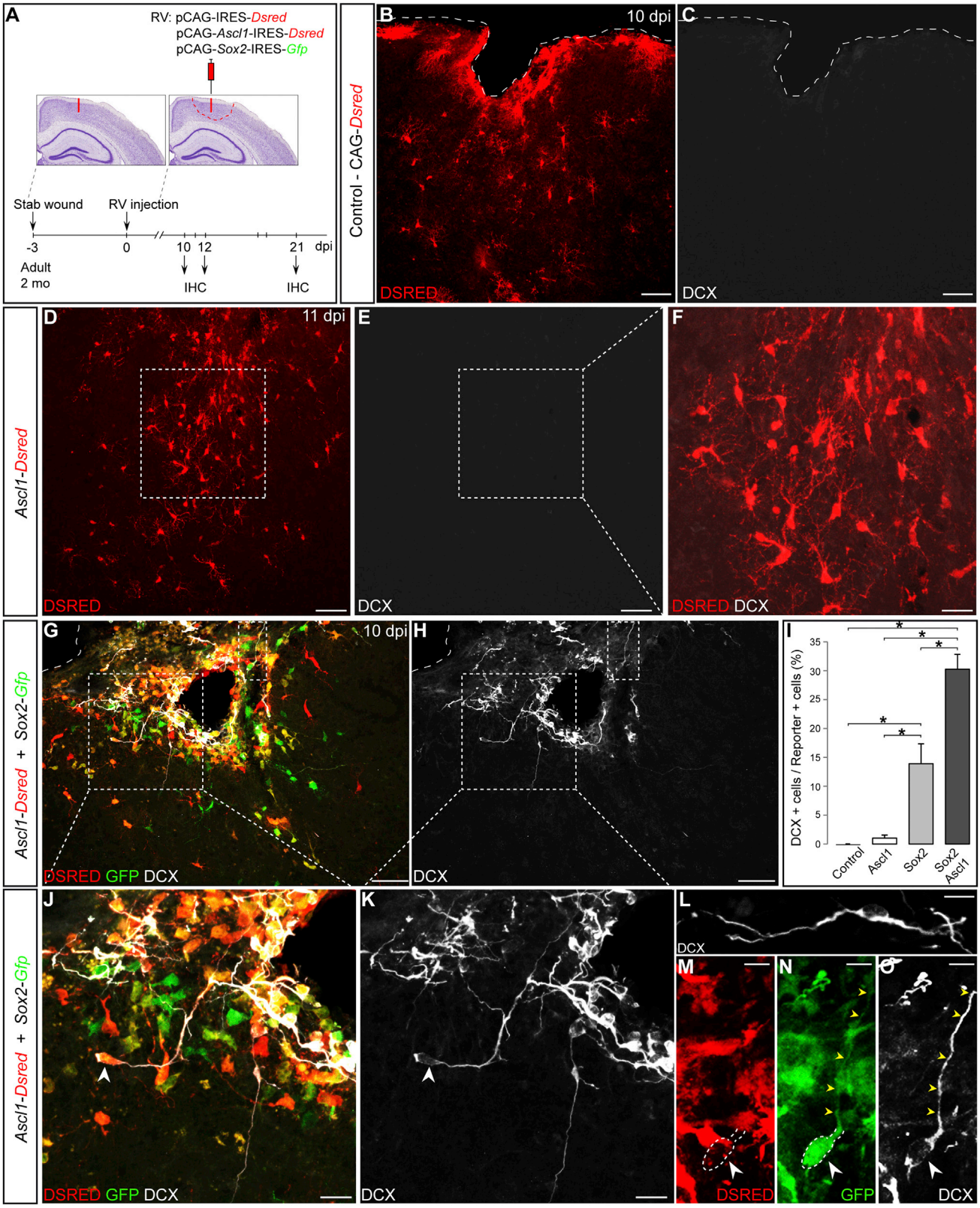

(legend on next page)

expression levels (Figures S3A–S3C). High SOX2 expression was often detected in transduced cells that were also DCX$^+$ (Figure S3D), suggesting that high SOX2 levels may not interfere but may be required for initial neuronal conversion.

A detailed analysis of the morphologies of *Sox2*-alone- or *Sox2*/*Ascl1*-induced neuronal cells revealed different degrees of complexity, highlighting a progressive maturation of induced neurons, not unlike previously described for adult-generated neurons in neurogenic zones (Bergami and Berninger, 2012). We found no statistically significant difference in the morphology of *Sox2*-alone- or *Sox2*/*Ascl1*-induced DCX$^+$ cells when grouping reporter$^+$/DCX$^+$ cells according to the complexity of their respective morphology (classes A–E; Figures 2O–2Q), albeit a tendency toward a more complex morphology was observed for *Sox2* and *Ascl1* coexpressing DCX$^+$ cells (*Sox2*: 258 DCX$^+$ cells analyzed, n = 4 mice; *Sox2*/*Ascl1*: 184 DCX$^+$ cells analyzed, n = 3 mice). Yet *Sox2*-alone-expressing cells were capable of acquiring complex neuronal morphologies (Figures 2E–2G and 2P), and some *Sox2*-induced neurons expressed the mature neuronal marker NeuN at 21 dpi (Figures 2H–2M). Albeit low in numbers, these NeuN$^+$ cells exhibited a highly complex neuronal morphology (Figure 2H) and had become DCX-negative (Figure 2N). Taken together, these data show that *Sox2* alone induces the conversion of nonneuronal cells into neurons in the injured adult mouse cortex.

Genetic Fate Mapping Demonstrates Reprogramming of NG2 Glia into Induced Neurons

Next, we aimed at identifying the cellular origin of the DCX$^+$ induced neurons. The above-mentioned quantification of the transduced cells following control retroviral injection revealed that the majority of the transduced cells were NG2 glia. To assess whether cells of the oligodendroglial lineage are those which convert into DCX$^+$ cells following forced expression of *Sox2* alone or *Sox2*/*Ascl1*, we used a bacterial artificial chromosome (BAC)-transgenic mouse line (Sox10-iCreER^{T2}/GFP) in which GFP reporter expression can be specifically induced upon tamoxifen-mediated recombination in cells with an active *Sox10* promoter and traced in their progeny, which are exclusively cells of the oligodendrocyte lineage, including NG2 glia and oligodendrocytes in the cerebral cortex (Simon et al., 2012).

Several weeks after genetic labeling of cells of the oligodendroglial lineage was induced by tamoxifen, adult transgenic mice received a stab wound lesion followed 3 days later by injection of retroviruses encoding *Sox2* and/or *Ascl1*, both containing a DSRED reporter. To determine the identity of fate-mapped cells following retroviral transduction, we performed immunostaining for GFP (identifying cells of oligodendroglial origin), DSRED (identifying transduced cells), and DCX (identifying induced neurons). Remarkably, the majority of DCX$^+$ cells following *Sox2* or *Sox2*/*Ascl1* expression were also GFP immunoreactive,

Figure 1. Induction of Neuronal Cells in the Injured Adult Cerebral Cortex upon Forced Expression of *Sox2* and *Ascl1*

(A) Schematic diagram of experimental procedures. The red bar shows the stab wound lesion restricted to the upper layers of the cortex. The red dashed line shows the area where cells transduced by retroviral vectors (RVs) are distributed. dpi, days postinjection; IHC, immunohistochemistry; mo, months.

(B and C) Absence of spontaneous neurogenesis in the injured adult cortex in control conditions. (B) The micrograph depicts DSRED$^+$ cells following injection of a control retrovirus encoding *Dsred* only (pCAG-IRES-*Dsred*) at 10 dpi. Most transduced cells exhibit a glial-like morphology. (C) Micrograph of the same field of view as shown in (B), revealing that neither transduced nor untransduced cells express DCX (white). The white dashed line marks the cortical surface.

(D–F) Virtual absence of induced neurogenesis in the injured adult cortex following forced expression of *Ascl1*. (D) The micrograph depicts DSRED$^+$ cells transduced by the retrovirus encoding *Ascl1* at 11 dpi (*Ascl1*-IRES-*Dsred*). Note the glial-like morphology of most transduced cells. (E) Micrograph of the same field of view as shown in (D), revealing that DSRED$^+$ transduced cells do not express DCX (white). (F) High-magnification view of the area boxed in (D) and (E), showing double immunostaining for DSRED and DCX (white).

(G–L) Forced expression of *Sox2* and *Ascl1* induces neurogenesis in the injured adult cortex. (G) Triple immunostaining for DSRED, GFP, and DCX reveals appearance of numerous induced neuronal cells expressing DCX (white) in the injured cortex following coexpression of *Sox2* (*Sox2*-IRES-*Gfp*) and *Ascl1* (*Ascl1*-IRES-*Dsred*), as shown at 10 dpi. (H) Micrograph of the same field of view as depicted in (G), showing the neuronal morphology of DCX$^+$ cells (white). (I) Numbers of induced reporter$^+$/DCX$^+$ neurons expressed as mean percentages ± SEM of the total number of transduced reporter$^+$ cells following injection of a retrovirus encoding *Dsred* only (control; n = 3 mice), *Ascl1* (n = 3 mice), *Sox2* (n = 4 mice), or *Sox2*/*Ascl1* (n = 3 mice). Statistical analysis was performed with Mann-Whitney U-test (*$p \leq 0.05$). (J and K) High-magnification views of the area boxed in (G) and (H), respectively, showing the density and neuronal morphology of DCX$^+$ cells (white). The arrowhead points to a DCX$^+$ cell extending a long and ramified process. (L) Example of a DCX$^+$ neuronal cell (white) induced upon expression of *Sox2* and *Ascl1*.

(M–O) Example of a DCX$^+$ neuron (white, arrowhead; O) boxed in (G) and (H), which appears to be induced by forced expression of *Sox2* only (green, arrowhead; N) in absence of *Ascl1* expression (red, arrowhead; M), as revealed by the white dashed line in (M) that mirrors the position of the depicted GFP$^+$ cell in (N). Yellow arrowheads indicate the neuronal process of the cell in (N) and (O).

The scale bars represent 60 μm (B–E), 25 μm (F), 55 μm (G and H), 17 μm (J and K), and 10 μm (L–O). See also Figures S1 and S2.

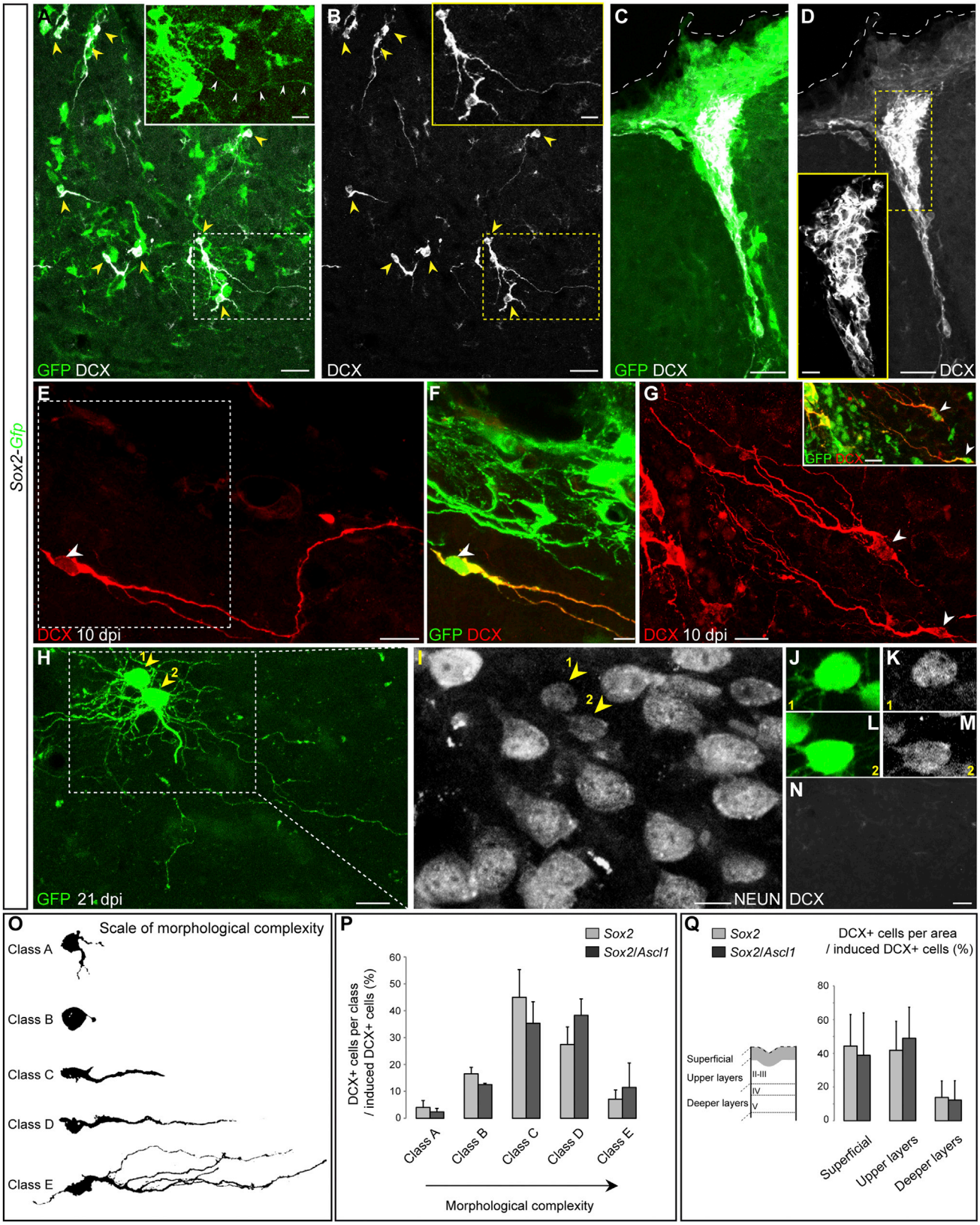

(legend on next page)

providing compelling evidence for an oligodendroglial origin of the induced neurons (59.8% ± 11.0% of DSRED$^+$/DCX$^+$ cells were also GFP$^+$ at 11.0 ± 0.6 dpi; 457 DCX$^+$ cells counted; n = 3 mice; Figures 3A–3F). Again, these GFP$^+$ and DCX$^+$ cells exhibited a characteristic morphology of immature neurons, indicating that forced *Sox2* or *Sox2*/*Ascl1* expression can convert proliferative cells of the oligodendroglial lineage into induced neurons. The fact that the responsive cells were targeted by a retrovirus and hence were proliferating at the time of injection excludes an oligodendrocyte origin of the DCX$^+$ cells, leaving NG2 glia as the main cellular source for induced neurons.

Induced Neuronal Cells Exhibit Voltage- and Time-Dependent Conductances and Receive Synaptic Inputs

To assess whether induced neuronal cells also exhibit neuronal membrane properties, we performed whole-cell patch-clamp recordings in acute slices obtained from cortices after stab wound lesion followed by coinjection with *Sox2*- and *Ascl1*-encoding retroviruses (n = 10 mice; 10–29 dpi; Figure 4A). Due to the damaged status of the tissue following stab wounding and viral injection and the presence of densely packed clusters of DSRED$^+$ cells (Figure S2A), DSRED$^+$ cells were selected randomly for recording. The majority of recorded cells lacked the ability of generating action potentials in response to step-current injections and were likely glial cells that failed to be converted into neurons (data not shown). More interestingly, several of the recorded cells exhibited early transient inward currents indicative of voltage- and time-dependent membrane conductances (Figures S4A–S4F). In some cases (2/17 cells), the recorded cells responded to depolarizing current injections with the generation of tetrodotoxin (TTX)-sensitive spike-like potential changes associated with TTX-sensitive inward sodium currents as revealed during voltage-clamp recordings (Figures 4B–4F). When cells were categorized according to absence or presence of voltage-gated conductances, the former group was characterized by low input resistance (~0.3 GΩ), whereas the latter exhibited relatively high input resistance values characteristic of immature neurons (≥1.2 GΩ; Table S1).

Next, we investigated whether transduced cells received functional synaptic inputs from surrounding neurons. A significant proportion of recorded cells (10/17 cells) exhibited spontaneous inward currents (Figures 4G and 4H), with an average amplitude of 15.0 ± 0.22 pA, a rise time of 1.2 ± 0.14 ms, and a decay time of 2.9 ± 0.33 ms, thus resembling spontaneous synaptic events (Figures 4G and 4H). Overall, the frequency of these synaptic currents was low (0.95 ± 0.22 events/min). These data indicate that a subset of *Sox2*- or *Sox2*/*Ascl1*-expressing cells possess functional neurotransmitter receptors and are capable of

Figure 2. Induction of Neuronal Cells in the Injured Adult Cerebral Cortex upon Forced Expression of *Sox2* Alone

(A–D) Forced expression of *Sox2* alone induces DCX$^+$ neurons in the injured adult cerebral cortex. (A) Double immunostaining for GFP and DCX reveals appearance of induced neurons expressing DCX (white) in the injured cortex following *Sox2* expression (*Sox2*-IRES-*Gfp*). Inset: high magnification of the boxed area showing GFP reporter expression in DCX$^+$ cells. (B) Micrograph of the same field of view as depicted in (A), showing the neuronal morphology of the DCX$^+$ cells (white, arrowheads). Inset: high magnification of the boxed area. (C and D) The micrographs depict a large cluster of densely packed DCX$^+$ cells (white) induced by forced expression of *Sox2* (green), located at the site of injury on top of the area depicted in (A) and (B). Inset in (D): high magnification of the boxed area (a single confocal plane is shown). (E–G) The micrographs depict DCX$^+$ neurons (red, arrowheads; E and F show the same cell) induced by forced expression of *Sox2* alone (green, F; inset in G) at 10 dpi. Note the high level of complexity and ramification of their neuronal processes.

(H–N) The micrographs depict two GFP$^+$/NeuN$^+$ neurons (arrowheads 1 and 2) at 21 dpi induced by forced expression of *Sox2* alone. (H) GFP immunostaining illustrating the high level of complexity and ramification of neuronal processes. (I) High-magnification view of the area boxed in (H), showing that these induced neurons express the mature neuronal marker NeuN (white, arrowheads 1 and 2). (J–M) High-magnification views showing GFP (J and L) and NeuN (K and M) immunoreactivity of the induced neurons (1 and 2). Single confocal optical planes are shown. (N) The micrograph shows the same field of view as shown in (H) and reveals loss of DCX expression in NeuN$^+$ mature neurons.

(O and P) Morphological maturation of neuronal cells induced by *Sox2* alone or *Sox2*/*Ascl1*. (O) Schematic diagram illustrating the progressive morphological maturation of DCX$^+$ induced neuronal cells that were categorized at ~12 dpi into five subsequent classes (A–E) according to their morphology. Class A: the cells are already DCX$^+$ although still exhibiting a glial-like morphology with several processes; class B: the cells round up loosing their processes and exhibit a cytoplasmic ring of DCX; class C: the cells extend a single major DCX$^+$ process, which is up to twice the size of their soma in length; class D: the cells extend a long unbranched DCX$^+$ process, which is more than three times the size of their soma in length; and class E: the cells display a complex morphology and extend long DCX$^+$ processes that show several ramifications. Reconstructions of reporter$^+$/DCX$^+$ cells based on the reporter signal are shown. (P) Numbers of *Sox2*- and *Sox2*/*Ascl1*-induced DCX$^+$ cells in each class (O), expressed as mean percentages ± SEM of the total number of induced DCX$^+$ cells at ~12 dpi. (Q) Location of *Sox2*- and *Sox2*/*Ascl1*-induced DCX$^+$ cells throughout the injured cortical layers at ~12 dpi. Numbers of DCX$^+$ cells in each location (i.e., superficial, upper, and deeper layers) expressed as mean percentages ± SEM of the total number of induced DCX$^+$ cells. *Sox2*: 258 DCX$^+$ cells analyzed; n = 4 mice. *Sox2*/*Ascl1*: 184 DCX$^+$ cells analyzed; n = 3 mice.

The scale bars represent 26 μm (A and B), 30 μm (C and D), 10 μm (E; I; and insets in A, B, and D), 6 μm (F), 15 μm (G and inset in G), and 20 μm (H and N). See also Figure S3 and Movie S1.

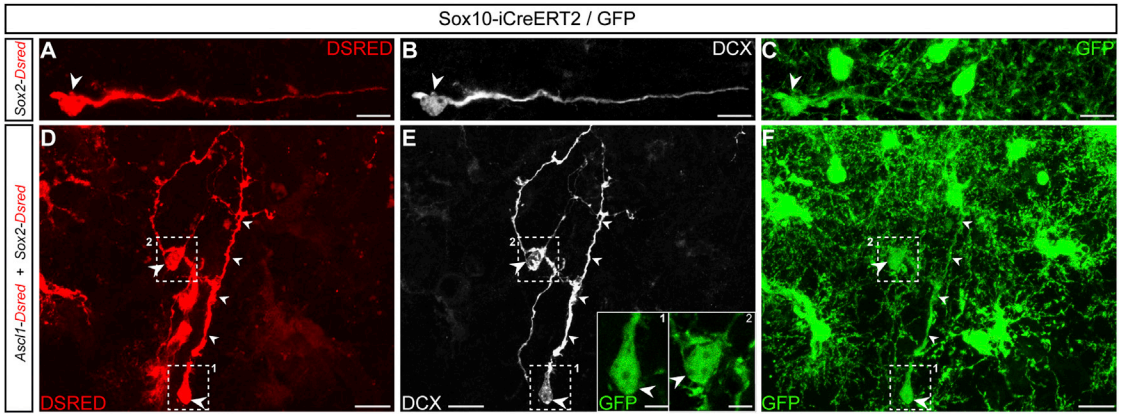

Figure 3. Genetic Fate Mapping Demonstrates Reprogramming of NG2 Glia into Induced Neurons

Following tamoxifen-induced recombination, Sox10-iCreER^{T2}/GFP mice received a stab wound injury followed 3 days later by injection of *Sox2*-encoding retrovirus (*Sox2*-IRES-*Dsred*; A–C) or two retroviruses encoding *Sox2* and *Ascl1* (*Ascl1*-IRES-*Dsred*; D–F).

(A–C) Neuronal conversion of fate-mapped NG2 glia upon *Sox2* expression. The micrographs depict a DSRED$^+$ transduced cell (A; 12 dpi) that is converted into a DCX$^+$ neuron (B, white) upon *Sox2* expression and is immunoreactive for GFP (C), demonstrating its oligodendroglial origin.

(D–F) Neuronal conversion of fate-mapped NG2 glia following coinjection of *Sox2*- and *Ascl1*-encoding retroviruses. The micrographs show two DSRED$^+$ transduced cells (D; 10 dpi; arrowheads) converted into DCX$^+$ neurons (E, white, arrowheads) that also express GFP (F, arrowheads). Insets in (E): high magnification of the boxed areas in (D–F) highlighting the GFP$^+$ soma of induced neurons (1 and 2). The scale bars represent 12 μm (A–F) and 4 μm (insets in E).

assembling a functional postsynaptic compartment. In line with these electrophysiological data, we observed spine-like protrusions on the processes of some DCX$^+$ cells (Figure 5A). Moreover, we also observed close appositions of GAD65/GAD67$^+$ puncta on the soma and processes of DCX$^+$ cells, suggesting the presence of presynaptic fibers from local interneurons impinging on induced neuronal cells (Figures 5B–5B″). Indeed, we found GFP$^+$ axonal varicosities wrapping around the soma and processes of induced DCX$^+$ cells in transgenic mice expressing GFP in a subpopulation of somatostatin$^+$ interneurons (Oliva et al., 2000) (n = 3 mice; Figures 5C–5H′). Together, these data are consistent with an immature neuronal identity of a substantial fraction of *Sox2*- or *Sox2*/*Ascl1*-expressing cells.

Sox2 Does Not Induce Neuronal Conversion of Glial Cells from the Cerebral Cortex in Absence of Stab Wound Injury

Because the majority of DCX$^+$ cells were located in close vicinity to the lesion area, we next asked whether changes in the cellular milieu induced by the stab wound lesion may be required for glia-to-neuron conversion. We performed injections of *Sox2*-encoding retrovirus in absence of prior stab wound injury. However, consistent with the fact that only NG2 glia proliferate in the healthy cerebral cortex with a very slow cell cycle (Dimou and Götz, 2014; Dimou et al., 2008), we did not detect a single GFP$^+$ transduced cell (n = 2 mice; data not shown).

We next injected *Sox2*-encoding lentivirus pseudotyped with the envelope proteins of Mokola or lymphocytic choriomeningitis virus (LCMV) viruses known to specifically target glial cells (Beyer et al., 2002; Buffo et al., 2005; Colin et al., 2009). We observed many GFP$^+$ cells distributed throughout all cortical layers and expressing high SOX2 levels (Figures 6A–6C). Virtually no GFP$^+$ cells showed the morphology of mature neurons, ruling out direct transduction of neurons by these lentiviruses (0.1% ± 0.1%; 2,261 GFP$^+$ cells counted; n = 3 mice; Colin et al., 2009). The vast majority of GFP$^+$ transduced cells exhibited the morphology of quiescent astrocytes as confirmed by immunoreactivity for S100β (Figures 6E and 6F; Mokola: 91.9% ± 0.7%, n = 2 mice; LCMV: 98.8%, n = 1 mouse). A small but substantial amount of GFP$^+$ cells displayed the morphology of NG2 glia and expressed OLIG2 (Figures 6G and 6H; Mokola: 7.9% ± 0.7%; LCMV: 1.2%). Figure 6I shows the pooled data from three mice following Mokola- or LCMV-pseudotyped lentivirus injection (94.2% ± 2.3% and 5.7% ± 2.3% of GFP$^+$ cells belonging to the astroglial and oligodendroglial lineage, respectively; 2,261 GFP$^+$ cells counted; n = 3 mice). However, despite the high rate of glia-specific transduction, virtually no DCX$^+$ cells could be observed (2,261 GFP$^+$ cells counted at 10 dpi; n = 3 mice; Figures 6D and 6I). As NG2 glia are the primary source for DCX$^+$ cells following forced *Sox2* expression in the stab-wound-lesioned cortex, we closely examined >100 GFP and OLIG2-double-positive cells, none of which were DCX

positive (0/132 cells; n = 3 mice). Of note, lentivirus-driven expression of *Sox2* induced appearance of DCX$^+$ cells in the context of cortical injury as observed before with the retroviral vector (Figure S5). These data suggest that prior lesion facilitates *Sox2*-induced conversion of NG2 glia.

DISCUSSION

Here, we provide evidence that the transcription factor *Sox2* alone or in combination with *Ascl1* is capable of inducing neurogenesis in the adult mouse cerebral cortex following traumatic injury. Genetic fate mapping revealed that the main cellular source of newly generated DCX$^+$ cells in this experimental paradigm belongs to the oligodendroglial lineage, although a minor contribution of astroglia cannot be excluded. In contrast, in the undamaged cerebral cortex, we failed to observe such response, suggesting that prior lesioning appears to be supportive for neuronal fate conversion.

Whereas most studies aiming at reprogramming brain-resident glia into neurons focused on astroglia, NG2 glia represent an interesting alternative cellular source given their abundance and life-long capacity for proliferation (Dimou and Götz, 2014). Here, we found that ~60% of the induced DCX$^+$ neurons derived from fate-mapped NG2 glia using Sox10-iCreER^{T2}/GFP transgenic mice. GFP-negative-induced neurons could either derive from non-fate-mapped NG2 glia (due to incomplete recombination) or originate from neuronal conversion of other glial cell types. However, we did not obtain evidence for astrocyte conversion into neurons using GLAST^{CreERT2}/GFP mice (Buffo et al., 2008; data not shown), suggesting that reactive astroglia play only a minor role as potential target cells in this experimental paradigm, consistent with the evidence that only a very small population of reactive astrocytes divide (Bardehle et al., 2013) or acquire stem cell potential after invasive stab wound injury (Buffo et al., 2008; Sirko et al., 2013). Intriguingly, however, Guo et al. (2014) reported conversion of reactive cortical astroglia by forced expression of *NeuroD1* using a mouse model with amyloidosis. This suggests that, in the injured brain, several cell populations may be amenable to reprogramming and that precise timing and factors employed may be critical in determining the outcome. Interestingly, NG2 glia exhibit enhanced proliferation in response to injury but remain committed to the oligodendroglial lineage (Dimou et al., 2008). Furthermore, Hughes et al. (2013) showed that these cells are recruited to sites of focal CNS injury. Thus, due to their enhanced proliferation and recruitment following injury, NG2 glia can be readily targeted by retroviruses at the injury site in vivo. Targeting this cell type for reprogramming may have the added benefit that replacement of converted NG2 glia may occur through homeostatic control of NG2 glia density (Hughes et al., 2013) and hence may not result in the exhaustion of the local NG2 glia pool. Retrovirus-mediated expression of *NeuroD1* under control of a human *NG2* promoter construct was also found to elicit neurogenesis in the cerebral cortex in vivo (Guo et al., 2014), providing independent evidence that NG2 glia can be reprogrammed into induced neurons.

Several groups recently reported on transcription-factor-driven fate conversion of local glial cells into induced neuronal cells (Arlotta and Berninger, 2014). Notably, there are major differences to our study with regard to the CNS areas studied, the health status of the tissue in which reprogramming was induced, the cell types targeted, and reprogramming factors used. Most studies employed well-characterized neurogenic transcription factors known to drive neuronal differentiation from neural stem/precursors cells (Buffo et al., 2005), including the proneural genes *Ascl1*, *Neurog2* (Grande et al., 2013; Torper et al., 2013), or *NeuroD1* (Guo et al., 2014). Albeit we initially followed the same logic of employing *Ascl1*, a well-known neuronal reprogramming factor (Berninger et al., 2007; Vierbuchen et al., 2010), forced *Ascl1* expression alone failed to induce any appreciable neurogenesis in our lesion paradigm. Our previous work suggested a synergistic enhancement of *Ascl1* reprogramming capacity by coexpression of *Sox2* (Karow et al., 2012). Whereas we could indeed observe a synergistic effect of these two factors on NG2 glia reprogramming, we were surprised that *Sox2* alone was sufficient to trigger de novo emergence of DCX$^+$ cells contrary to the notion that *Sox2* prevents neuronal differentiation from neural stem cells. Notably, a similar capacity of *Sox2* to convert astrocytes in the adult striatum and spinal cord into DCX$^+$ cells was recently reported (Niu et al., 2013; Su et al., 2014), providing independent evidence for this unexpected capacity of *Sox2* to induce a glia-to-neuron fate switch. Interestingly, whereas we do not have direct evidence for continued proliferation, we observed clusters of *Sox2*-induced DCX$^+$ cells in agreement with Niu et al. (2013). If continued proliferation turns out to be a characteristic feature of *Sox2*-induced glia reprogramming, this may allow for a local amplification of the pool of induced neurons.

Expression of *Sox2* alone was sufficient to induce neurogenesis without requirement for coexpression of a proneural transcription factor. This is surprising, as *Sox2* function in neural stem cells is to promote self-renewal rather than neuronal differentiation (Graham et al., 2003; Pevny and Nicolis, 2010) and *Sox2* may even convert fibroblasts into multipotent neural stem cells (Ring et al., 2012). Whereas these reports highlight the role of *Sox2* in neural stem/progenitor cells, *Sox2*-induced conversion of CD133$^+$ cord blood cells into neuronal cells was also described in vitro (Giorgetti et al., 2012). Of note, Kondo and Raff (2000,

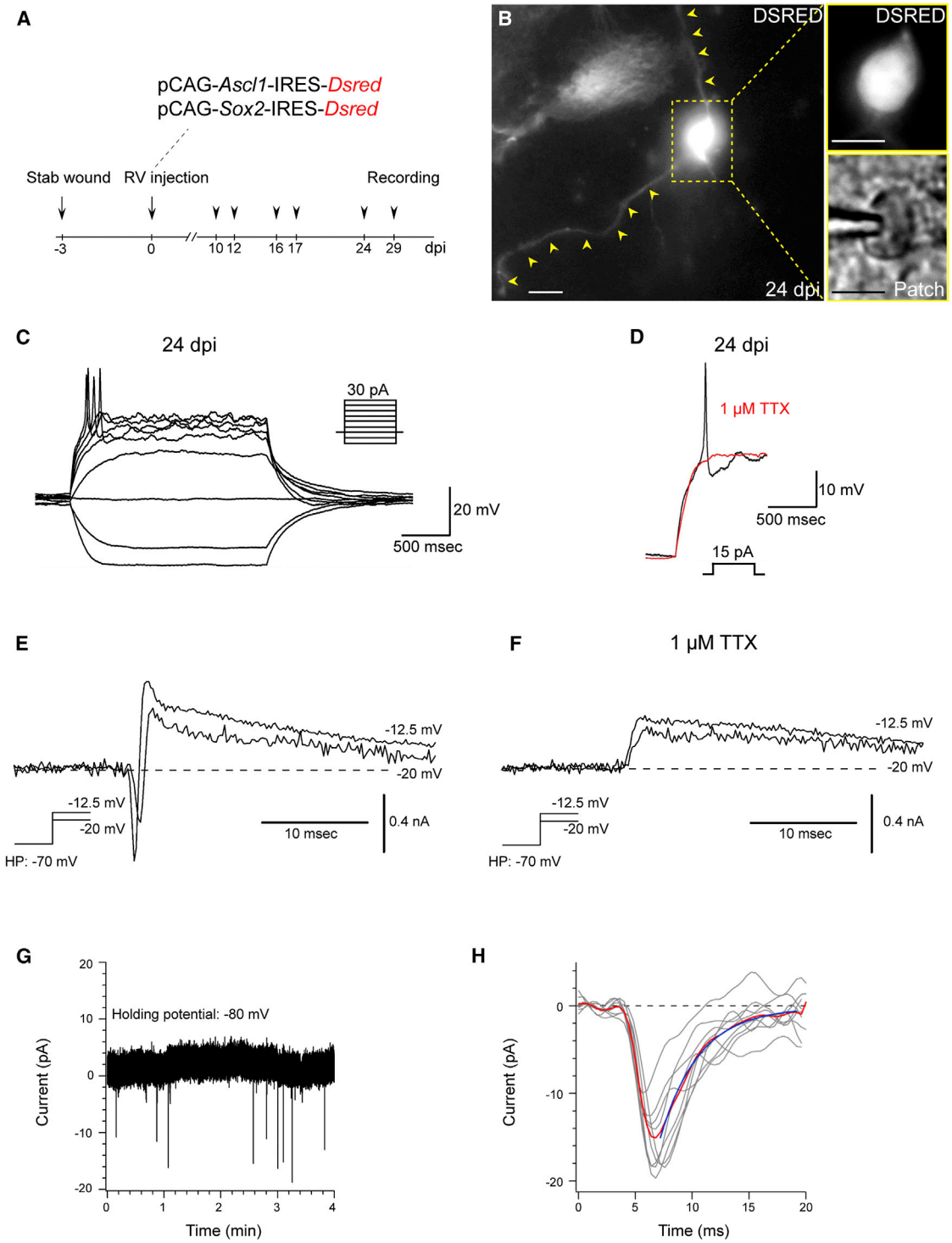

Figure 4. Induced Neuronal Cells Exhibit Voltage- and Time-Dependent Conductances and Receive Synaptic Inputs

(A) Schematic diagram of experimental design.

(B) The micrograph depicts an example of DSRED$^+$ cell 24 days after coinjection of *Sox2*- (*Sox2*-IRES-*Dsred*) and *Ascl1* (*Ascl1*-IRES-*Dsred*)-encoding retroviruses, exhibiting a neuronal morphology selected for patch-clamp recording. Arrowheads point to processes emerging from the cell body. Insets: DSRED fluorescence and bright field picture of the cell body with the patch pipette.

(legend continued on next page)

2004) observed that growth-factor-induced conversion of cultured OPCs into multipotent neural-stem-cell-like cells was accompanied by the reactivation of the *Sox2* gene. However, Niu et al. (2013) provided evidence against a neural stem cell intermediate that would precede *Sox2*-induced neurogenesis in the adult striatum.

Intriguingly, lentivirus-mediated expression of *Sox2* failed to elicit appreciable induction of DCX$^+$ cells in the noninjured cerebral cortex. In the striatum, however, successful glia-to-neuroblast conversion could be achieved without injury (Niu et al., 2013), suggesting differences in the reprogramming permissiveness of cortical versus striatal glia (see also Buffo et al., 2005; Kronenberg et al., 2010). Possible reasons for the injury-induced facilitation of *Sox2*-mediated reprogramming may lie in the mild upregulation of some neurogenic factors or the accelerated cell cycle of NG2 glia following cortical injury (Dimou and Götz, 2014), which may render NG2 glia more permissive to chromatin remodelling required for fate conversion. Additionally, cytokines, growth factors, and morphogens released upon injury may directly impinge on reprogramming mechanisms, as activation or interference with these signaling pathways can dramatically enhance fate conversion into neurons (Grande et al., 2013; Ladewig et al., 2012).

Whereas a small fraction of the *Sox2*-induced DCX$^+$ cells appeared to develop into more mature neurons as characterized by NeuN immunoreactivity and a highly complex morphology, most cells failed to acquire neuronal-subtype-specific traits as detected by immunohistochemistry for class-specific transcription factors or the machinery for neurotransmitter release (e.g., TBR1, NKX 2.1, GABA, and GAD65/GAD67; data not shown). This indicates that the majority of DCX$^+$ cells may remain trapped in an immature state. This is in line with the study by Niu et al. (2013), although we did not note the necessity for terminating *Sox2* expression for successful emergence of DCX$^+$ cells. Intriguingly, Niu and colleagues showed that treatment with the neurotrophin *Bdnf* and the bone morphogenetic protein inhibitor *Noggin* or with the histone deacetylase inhibitor valproic acid can release these cells from the apparent break that prevents further neuronal maturation. Indeed, following such treatments, *Sox2*-induced neurons acquired the ability of generating trains of action potentials (Niu et al., 2013).

In our study, the electrophysiological analysis revealed that some cells following transduction with *Sox2*- and/or *Ascl1*-encoding viruses exhibited voltage- and time-dependent conductances and, in some cases, elicited voltage changes resembling action potentials. This is consistent with the fact that the majority of reprogrammed cells remain immature. However, in the electrophysiological analysis, we were unable to select only successfully reprogrammed cells, and most cells exhibiting properties of nonexcitable cells were likely glia that failed to undergo reprogramming. More interestingly, ~60% of the recorded cells received synaptic inputs, albeit at low frequency. As shown in GFP-expressing inhibitory neurons (GIN) mice, some of these inputs may arise from GABAergic interneurons. Whereas this indicates some degree of functional integration of these transduced cells, at the current state, it is unclear whether this reflects de novo acquisition of synaptic contacts following neuronal conversion or maintenance of synapses established onto these cells while still being NG2 glia. In fact, NG2 glia were shown to receive synaptic inputs from glutamatergic and GABAergic neurons (Bergles et al., 2000; Lin and Bergles, 2004) and retain these even during cell division (Ge et al., 2009). Whereas the electrophysiological features of our recorded cells cannot be taken as evidence for de novo acquisition of synaptic contacts, synaptic innervation may be an important factor contributing to the reprogramming process and may be relevant when considering strategies to improve maturation and functional integration of induced DCX$^+$ neurons.

In summary, this study revealed the unexpected capacity of *Sox2* for converting reactive glial cells into induced DCX$^+$ neurons in the injured cerebral cortex. Our work highlights the potential of NG2 glia as cellular candidates for de novo generation of new neurons in the cerebral cortex, a brain area otherwise totally devoid of neurogenesis. Future studies aiming at improving maturation of the newly generated neuronal cells are required to fully reveal the potential of such fate conversion for brain repair.

(C) Ability of a DSRED$^+$ cell to generate action-potential-like voltage changes in response to depolarizing current injection. Changes in membrane potential in response to de- and hyperpolarizing currents are shown.
(D) The action-potential-like signals induced by suprathreshold current pulses are blocked by TTX (red trace).
(E and F) Voltage-clamp recording of the same DSRED$^+$ cell as shown in (D), demonstrating the presence of a Na$^+$ current blocked by TTX. (E) Two current traces recorded in absence of TTX and at the indicated command potentials are shown. Holding potential (HP): −70 mV; step potential duration: 300 ms. Traces are depicted superimposed. (F) Similar recordings in the same cell following application of TTX. Currents were corrected for leakage currents.
(G and H) Examples of spontaneously occurring synaptic inputs recorded in a DSRED$^+$ transduced cell. (G) A voltage-clamp recording for 4 min is shown. Nine synaptic-event-like responses are identified. (H) Events detected in (G) were superimposed with respect to their onset and averaged (red trace). Blue line: monoexponential fit to the average decay of these events.
The scale bars represent 10 μm (B, insets). See also Figure S4 and Table S1.

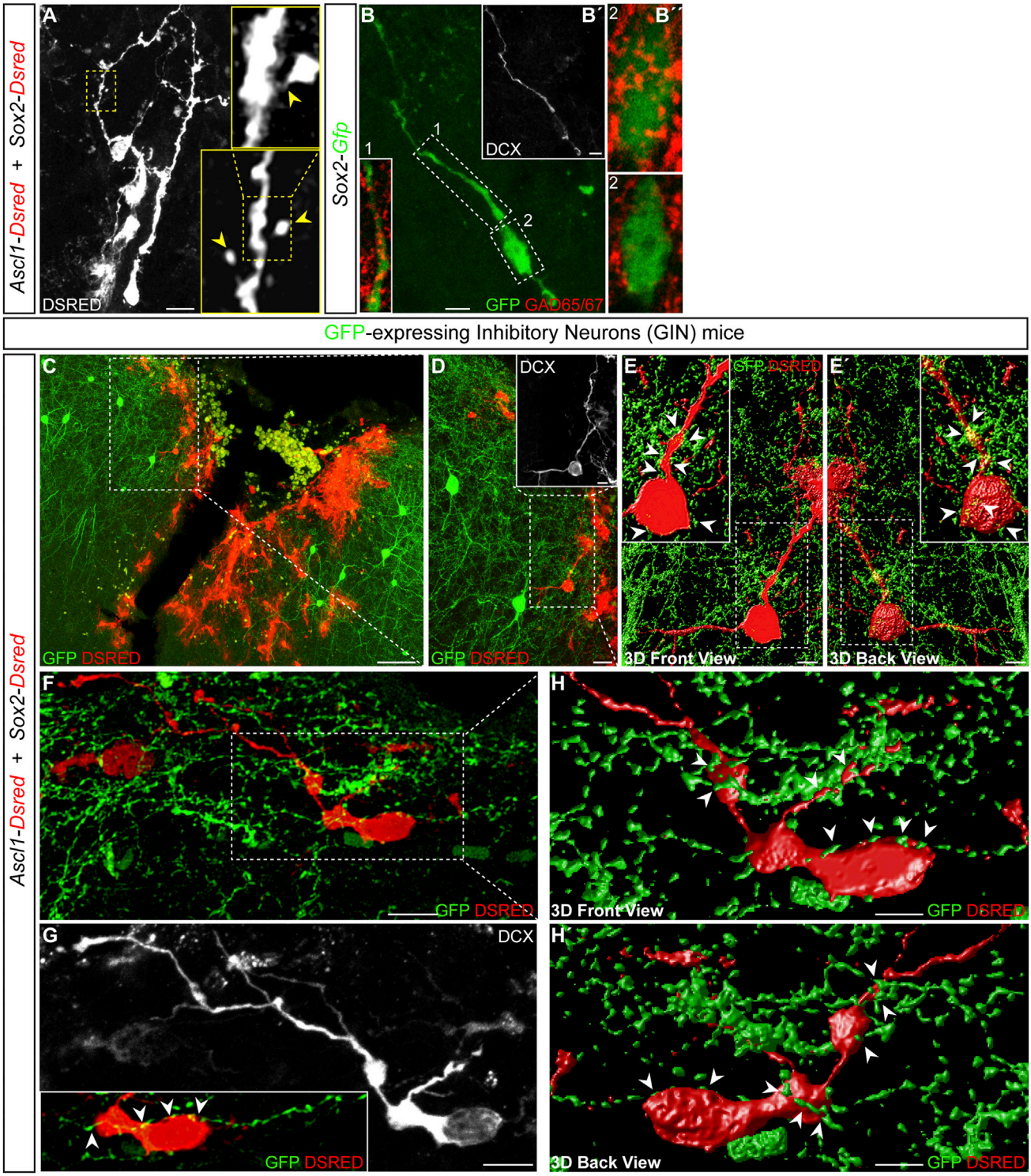

Figure 5. Induced Neurons Receive Synaptic Connections from Endogenous GABAergic Neurons

(A) The micrograph shows DSRED$^+$-induced neurons following coinjection of *Sox2*- and *Ascl1*-encoding retroviruses (the same cells are also shown in Figure 3D). Lower inset: high magnification of the boxed area showing some spine-like protrusions on the process of the DCX$^+$ neuron (arrowheads). Upper inset: zoomed view of the area boxed in the lower inset showing the neck of one spine-like protrusion (arrowhead; a single confocal plane is shown).

(legend continued on next page)

EXPERIMENTAL PROCEDURES

Animals

Experiments were conducted on adult C57BL/6J mice (8–10 weeks old). Sox10-iCreER^{T2}/GFP or GLAST^{CreERT2}/GFP mice were used for fate-mapping studies (Buffo et al., 2008; Simon et al., 2012) and GIN mice (Oliva et al., 2000) for cortical interneuron monitoring. Animal procedures were carried out in accordance with policies of use of Animals and Humans in Neuroscience Research, revised and approved by the Society of Neuroscience and the Bavarian state. All efforts were made to minimize animal suffering and to reduce animal numbers.

Stab Wound Lesion

Adult mice received a stab wound lesion in the cerebral cortex as previously described (Buffo et al., 2005) by inserting a thin knife into the cortical parenchyma at the following coordinates: anteroposterior: −2; mediolateral: −1.6 with bregma as reference; and dorsoventral: −0.5 mm from dura. To produce stab lesions, the knife was moved over ~1 mm back and forth along the anteroposterior axis from −1.6 to −2.5 mm. Further details are given in the Supplemental Experimental Procedures.

Stereotactic Virus Injection

Three days after stab-wound injury, the same animals were injected with a viral suspension in the injured cortex within the stab wound area (depth: −0.5 mm from dura). C57BL/6J mice received (1) a mixture (1:1 ratio) of two retroviral vectors encoding *Ascl1* (pCAG-*Ascl1*-IRES-*Dsred*) and *Sox2* (pCAG-*Sox2*-IRES-*Gfp*), (2) a single retroviral vector encoding *Ascl1*, (3) a single retroviral (or lentiviral) vector encoding *Sox2*, or (4) a retroviral vector encoding *Dsred* only (pCAG-IRES-*Dsred*) for controls. For patch-clamp recording, C57BL/6J mice were injected with a mixture of two retroviruses encoding *Ascl1* (pCAG-*Ascl1*-IRES-*Dsred*) and *Sox2* (pCAG-*Sox2*-IRES-*Dsred*). GIN, Sox10-iCreER^{T2}/GFP, and GLAST^{CreERT2}/GFP mice received an injection of either *Ascl1*- and *Sox2*-encoding retroviruses or *Sox2*-encoding virus alone, both viruses containing a DSRED reporter.

In absence of stab wound injury, C57BL/6J mice were injected with a viral suspension in the cerebral cortex as described (Motori et al., 2013). A portion of the skull over the somatosensory cortex was thinned with a dental drill. A syringe needle was used to carefully create a small perforation of the skull. A thin glass capillary containing the virus was inserted through the microperforation (−0.5 mm from dura). Animals received a retroviral vector or a Mokola- or LCMV-pseudotyped lentiviral vector encoding *Sox2* (pCAG-*Sox2*-IRES-*Gfp*). Further details are given in the Supplemental Experimental Procedures.

A detailed description of tamoxifen treatment, bromodeoxyuridine labeling, electrophysiology, histological procedures, cell quantifications, and statistical analysis is provided in the Supplemental Experimental Procedures.

SUPPLEMENTAL INFORMATION

Supplemental Information includes Supplemental Experimental Procedures, five figures, one table, and one movie and can be found with this article online at http://dx.doi.org/10.1016/j.stemcr.2014.10.007.

AUTHOR CONTRIBUTIONS

C.H. made the original observation of Sox2-mediated conversion of NG2 glia into neurons. C.H. designed, conducted, and analyzed the majority of the in vivo reprogramming experiments. C.H. and M.B. analyzed the synaptic innervation of reprogrammed cells. M.B. and B.S. performed the patch-clamp experiments and analyzed the data. S.G. designed the lentivirus encoding Sox2.

(B–B″) Close apposition of GAD65/GAD67$^+$ puncta on the soma and processes of DCX$^+$ induced neurons. (B) The micrograph depicts a GFP$^+$ neuron induced by forced expression of *Sox2* at 11 dpi. Inset: High-magnification view of the area no. 1 boxed in (B), showing several GAG65/GAG67$^+$ puncta (red) in close apposition with the GFP$^+$ process of the induced neuron. (B′) Same field of view as shown in (B), revealing DCX immunoreactivity of the GFP$^+$ transduced cell. (B″) High-magnification views of the area no. 2 boxed in (B), showing several GAG65/GAG67$^+$ puncta (red) in close apposition with the GFP$^+$ soma of the induced neuron. Upper panel: single confocal plane of the top of the cell revealing several puncta distributed on the cell surface. Lower panel: single optical confocal plane sectioning the cell in its middle, revealing the presence of puncta located around the cell body.

(C–H′) GFP$^+$ axonal fibers and varicosities originating from GABAergic neurons wrap around the soma and processes of DCX$^+$ induced neurons at 23 dpi. (C) GFP-expressing inhibitory neurons (GIN) transgenic mice received a coinjection of *Sox2*- and *Ascl1*-encoding retrovirus 3 days after stab-wound injury. The micrograph shows an overview of the stab-wounded area with the majority of DSRED$^+$ transduced cells being located within the injured area, whereas several GFP$^+$ GABAergic neurons are located on both sides of the lesion. Note the presence of several GFP$^+$-intermingled dendritic and axonal processes. (D) High magnification of the area boxed in (C), depicting a DSRED$^+$-induced neuron surrounded by GFP$^+$ endogenous GABAergic interneurons and their processes. Inset: zoomed view of the area boxed in (D), illustrating the DCX immunoreactivity (white) of this induced neuron. (E and E′) 3D reconstruction of the same induced neuron shown in (D) (boxed area), depicting GFP$^+$ axonal varicosities impinging on its soma and processes, arguing for innervation by local interneurons (arrowheads). 3D front (E) and back (E′) views are shown. Insets in (E and E′): high-magnification views of the area boxed in (E) and (E′). (F–H′) Example of another close apposition of GFP$^+$ axons and axonal varicosities on the soma and processes of a DSRED$^+$-induced neuron (F; arrowheads in H and H′). (G) High magnification of the same neuron depicted in (F), illustrating its DCX immunoreactivity (white). Inset: magnified view of a GFP$^+$ axonal fiber and its varicosities wrapping around the induced neuron (arrowheads). (H and H′) 3D reconstruction of the same neuron shown in (F) (boxed area) and (G). 3D front (H) and back (H′) views are shown.

The scale bars represent 10 μm (A), 6 μm (B and B′), 70 μm (C), 14 μm (D), 7 μm (inset in D), 5 μm (E and E′), 9 μm (F), 7 μm (G), and 3.5 μm (H and H′).

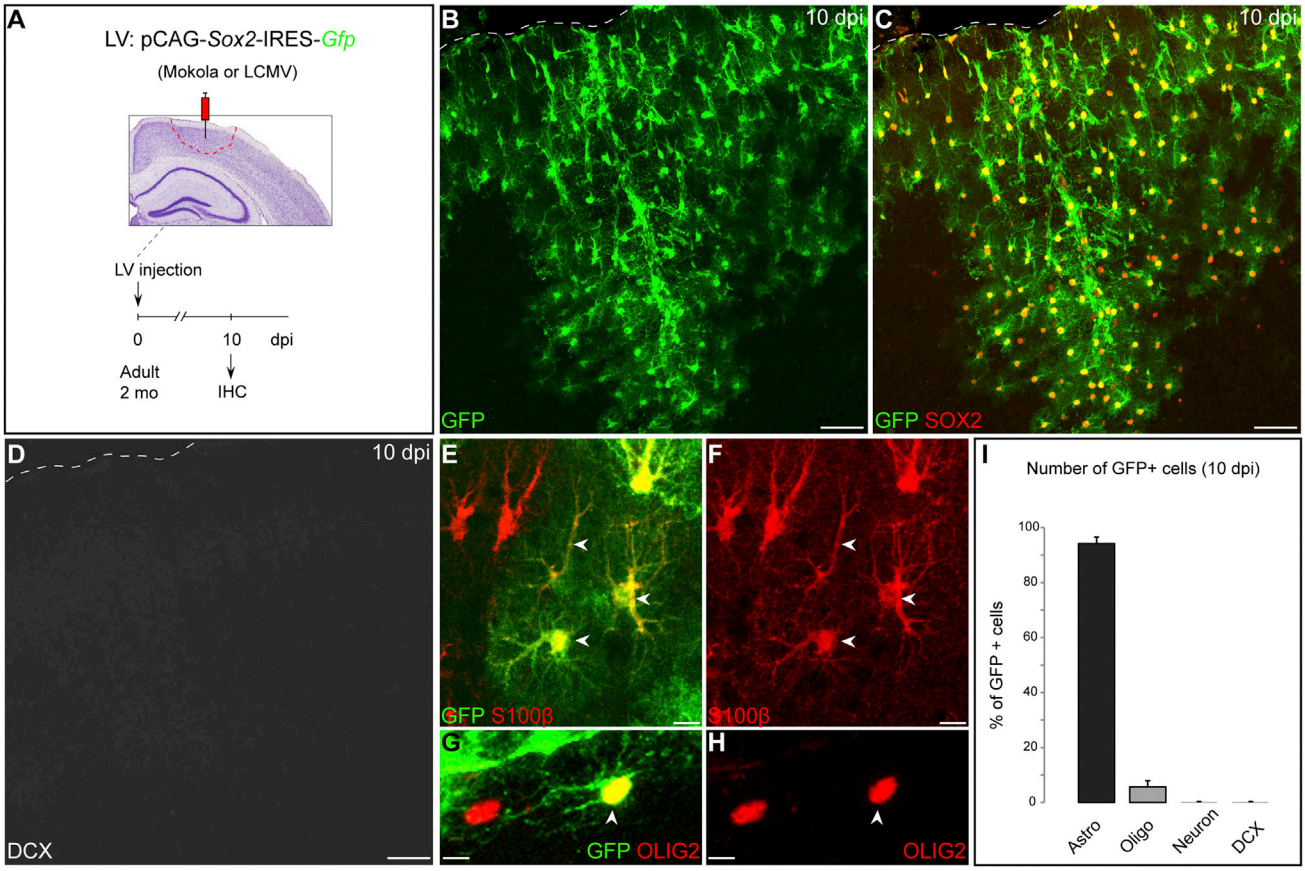

Figure 6. Forced Expression of *Sox2* Does Not Induce Neuronal Conversion of Cortical Glial Cells in Absence of Stab Wound Injury

(A) Schematic diagram of experimental procedures. The red dashed line shows the area where cells transduced by the lentiviral vector are distributed.

(B–D) Absence of neurogenesis induced by forced expression of *Sox2* in the noninjured adult cortex. (B) The micrograph depicts GFP$^+$ cells following injection of a Mokola-pseudotyped lentivirus encoding *Sox2* expression (*Sox2*-IRES-*Gfp*) at 10 dpi. Most transduced cells exhibit a glial morphology. (C) Micrograph of the same field of view as shown in (B), revealing high levels of SOX2 expression (red) in all GFP$^+$ transduced cells. (D) Micrograph of the same field of view as shown in (B) and (C), depicting that none of the transduced cells is DCX$^+$ (white).

(E–H) GFP$^+$ transduced cells are astrocytes and NG2 glia. (E and F) Double immunostaining for GFP and S100β (red), showing astrocytes transduced by the lentivirus (arrowheads). (G and H) Double immunostaining for GFP and OLIG2 (red), showing one transduced cell of the oligodendroglial lineage (arrowhead).

(I) Numbers of GFP$^+$ cells in each category (i.e., astro, oligo, neuron, and DCX) are expressed as mean percentages ± SEM of the total number of transduced GFP$^+$ cells following injection of the Mokola- or LCMV-pseudotyped lentiviruses encoding *Sox2* (pooled data; n = 3 mice).

The scale bars represent 70 μm (B–D), 12 μm (E and F), and 6 μm (G and H). See also Figure S5.

A.L. designed and produced the majority of viral vectors used in the present study. F.V. contributed to the histology. L.D. provided advice regarding the fate-mapping experiments and provided the Sox10-iCreERT2 mice. M.G. initiated and financed the project. B.B. and M.G. supervised the project. C.H., B.B., and M.G. wrote the manuscript. All authors discussed the manuscript.

ACKNOWLEDGMENTS

We thank Dr. M. Wernig (Stanford University) for the *Sox2* sequence and Dr. C. Lie (Erlangen University) for the *Sox2* viral vector. We are grateful to Dr. G. Masserdotti and Dr. M. Karow for help with the viral vector cloning and production. We are grateful to G. Jaeger for excellent technical assistance and to I. Mühlhahn and D. Franzen for virus production. We thank A. von Streitberg for oral gavaging of the animals with tamoxifen. This work was supported by grants from the SPP1356 (BE 4182/2-2 and GO 640/9-2) of the DFG, the BMBF (01GN1009A and 01GN0976), the Bavarian State Ministry of Sciences, Research and the Arts (ForNeuroCell) to B.B. and M.G., the Belgian Science Policy Office (P7/20 Wibrain) to B.B., and BMBF and DFG grants (GO640/6-1, 7-1, and 8-1) to M.G. We are indebted to the Collaborative Research

Center 870 funded by the DFG for financing the viral vector facility. M.B. was funded by the LMU Research fellowship program.

Received: July 31, 2013
Revised: October 16, 2014
Accepted: October 16, 2014
Published: November 20, 2014

REFERENCES

Arlotta, P., and Berninger, B. (2014). Brains in metamorphosis: reprogramming cell identity within the central nervous system. Curr. Opin. Neurobiol. *27C*, 208–214.

Bardehle, S., Kruger, M., Buggenthin, F., Schwausch, J., Ninkovic, J., Clevers, H., Snippert, H.J., Theis, F.J., Meyer-Luehmann, M., Bechmann, I., et al. (2013). Live imaging of astrocyte responses to acute injury reveals selective juxtavascular proliferation. Nat. Neurosci. *16*, 580–586.

Bergami, M., and Berninger, B. (2012). A fight for survival: the challenges faced by a newborn neuron integrating in the adult hippocampus. Dev. Neurobiol. *72*, 1016–1031.

Bergles, D.E., Roberts, J.D., Somogyi, P., and Jahr, C.E. (2000). Glutamatergic synapses on oligodendrocyte precursor cells in the hippocampus. Nature *405*, 187–191.

Berninger, B., Costa, M.R., Koch, U., Schroeder, T., Sutor, B., Grothe, B., and Götz, M. (2007). Functional properties of neurons derived from in vitro reprogrammed postnatal astroglia. J. Neurosci. *27*, 8654–8664.

Beyer, W.R., Westphal, M., Ostertag, W., and von Laer, D. (2002). Oncoretrovirus and lentivirus vectors pseudotyped with lymphocytic choriomeningitis virus glycoprotein: generation, concentration, and broad host range. J. Virol. *76*, 1488–1495.

Buffo, A., Vosko, M.R., Erturk, D., Hamann, G.F., Jucker, M., Rowitch, D., and Götz, M. (2005). Expression pattern of the transcription factor Olig2 in response to brain injuries: implications for neuronal repair. Proc. Natl. Acad. Sci. USA *102*, 18183–18188.

Buffo, A., Rite, I., Tripathi, P., Lepier, A., Colak, D., Horn, A.P., Mori, T., and Götz, M. (2008). Origin and progeny of reactive gliosis: A source of multipotent cells in the injured brain. Proc. Natl. Acad. Sci. USA *105*, 3581–3586.

Colin, A., Faideau, M., Dufour, N., Auregan, G., Hassig, R., Andrieu, T., Brouillet, E., Hantraye, P., Bonvento, G., and Deglon, N. (2009). Engineered lentiviral vector targeting astrocytes in vivo. Glia *57*, 667–679.

Dimou, L., and Götz, M. (2014). Glial cells as progenitors and stem cells: new roles in the healthy and diseased brain. Physiol. Rev. *94*, 709–737.

Dimou, L., Simon, C., Kirchhoff, F., Takebayashi, H., and Götz, M. (2008). Progeny of Olig2-expressing progenitors in the gray and white matter of the adult mouse cerebral cortex. J. Neurosci. *28*, 10434–10442.

Gage, F.H., and Temple, S. (2013). Neural stem cells: generating and regenerating the brain. Neuron *80*, 588–601.

Ge, W.P., Zhou, W., Luo, Q., Jan, L.Y., and Jan, Y.N. (2009). Dividing glial cells maintain differentiated properties including complex morphology and functional synapses. Proc. Natl. Acad. Sci. USA *106*, 328–333.

Giorgetti, A., Marchetto, M.C., Li, M., Yu, D., Fazzina, R., Mu, Y., Adamo, A., Paramonov, I., Cardoso, J.C., Monasterio, M.B., et al. (2012). Cord blood-derived neuronal cells by ectopic expression of Sox2 and c-Myc. Proc. Natl. Acad. Sci. USA *109*, 12556–12561.

Graham, V., Khudyakov, J., Ellis, P., and Pevny, L. (2003). SOX2 functions to maintain neural progenitor identity. Neuron *39*, 749–765.

Grande, A., Sumiyoshi, K., Lopez-Juarez, A., Howard, J., Sakthivel, B., Aronow, B., Campbell, K., and Nakafuku, M. (2013). Environmental impact on direct neuronal reprogramming in vivo in the adult brain. Nat. Commun. *4*, 2373.

Guo, Z., Zhang, L., Wu, Z., Chen, Y., Wang, F., and Chen, G. (2014). In Vivo direct reprogramming of reactive glial cells into functional neurons after brain injury and in an Alzheimer's disease model. Cell Stem Cell *14*, 188–202.

Heinrich, C., Blum, R., Gascon, S., Masserdotti, G., Tripathi, P., Sanchez, R., Tiedt, S., Schroeder, T., Götz, M., and Berninger, B. (2010). Directing astroglia from the cerebral cortex into subtype specific functional neurons. PLoS Biol. *8*, e1000373.

Heins, N., Malatesta, P., Cecconi, F., Nakafuku, M., Tucker, K.L., Hack, M.A., Chapouton, P., Barde, Y.A., and Götz, M. (2002). Glial cells generate neurons: the role of the transcription factor Pax6. Nat. Neurosci. *5*, 308–315.

Hughes, E.G., Kang, S.H., Fukaya, M., and Bergles, D.E. (2013). Oligodendrocyte progenitors balance growth with self-repulsion to achieve homeostasis in the adult brain. Nat. Neurosci. *16*, 668–676.

Karow, M., Sanchez, R., Schichor, C., Masserdotti, G., Ortega, F., Heinrich, C., Gascon, S., Khan, M.A., Lie, D.C., Dellavalle, A., et al. (2012). Reprogramming of pericyte-derived cells of the adult human brain into induced neuronal cells. Cell Stem Cell *11*, 471–476.

Kondo, T., and Raff, M. (2000). Oligodendrocyte precursor cells reprogrammed to become multipotential CNS stem cells. Science *289*, 1754–1757.

Kondo, T., and Raff, M. (2004). Chromatin remodeling and histone modification in the conversion of oligodendrocyte precursors to neural stem cells. Genes Dev. *18*, 2963–2972.

Kronenberg, G., Gertz, K., Cheung, G., Buffo, A., Kettenmann, H., Götz, M., and Endres, M. (2010). Modulation of fate determinants Olig2 and Pax6 in resident glia evokes spiking neuroblasts in a model of mild brain ischemia. Stroke *41*, 2944–2949.

Ladewig, J., Mertens, J., Kesavan, J., Doerr, J., Poppe, D., Glaue, F., Herms, S., Wernet, P., Kogler, G., Muller, F.J., et al. (2012). Small molecules enable highly efficient neuronal conversion of human fibroblasts. Nat. Methods *9*, 575–578.

Lin, S.C., and Bergles, D.E. (2004). Synaptic signaling between GABAergic interneurons and oligodendrocyte precursor cells in the hippocampus. Nat. Neurosci. *7*, 24–32.

Motori, E., Puyal, J., Toni, N., Ghanem, A., Angeloni, C., Malaguti, M., Cantelli-Forti, G., Berninger, B., Conzelmann, K.K., Götz, M., et al. (2013). Inflammation-induced alteration of astrocyte

mitochondrial dynamics requires autophagy for mitochondrial network maintenance. Cell Metab. *18*, 844–859.

Ninkovic, J., Steiner-Mezzadri, A., Jawerka, M., Akinci, U., Masserdotti, G., Petricca, S., Fischer, J., von Holst, A., Beckers, J., Lie, C.D., et al. (2013). The BAF complex interacts with Pax6 in adult neural progenitors to establish a neurogenic cross-regulatory transcriptional network. Cell Stem Cell *13*, 403–418.

Niu, W., Zang, T., Zou, Y., Fang, S., Smith, D.K., Bachoo, R., and Zhang, C.L. (2013). In vivo reprogramming of astrocytes to neuroblasts in the adult brain. Nat. Cell Biol. *15*, 1164–1175.

Ohira, K., Furuta, T., Hioki, H., Nakamura, K.C., Kuramoto, E., Tanaka, Y., Funatsu, N., Shimizu, K., Oishi, T., Hayashi, M., et al. (2010). Ischemia-induced neurogenesis of neocortical layer 1 progenitor cells. Nat. Neurosci. *13*, 173–179.

Oliva, A.A., Jr., Jiang, M., Lam, T., Smith, K.L., and Swann, J.W. (2000). Novel hippocampal interneuronal subtypes identified using transgenic mice that express green fluorescent protein in GABAergic interneurons. J. Neurosci. *20*, 3354–3368.

Pevny, L.H., and Nicolis, S.K. (2010). Sox2 roles in neural stem cells. Int. J. Biochem. Cell Biol. *42*, 421–424.

Ring, K.L., Tong, L.M., Balestra, M.E., Javier, R., Andrews-Zwilling, Y., Li, G., Walker, D., Zhang, W.R., Kreitzer, A.C., and Huang, Y. (2012). Direct reprogramming of mouse and human fibroblasts into multipotent neural stem cells with a single factor. Cell Stem Cell *11*, 100–109.

Robel, S., Berninger, B., and Götz, M. (2011). The stem cell potential of glia: lessons from reactive gliosis. Nat. Rev. Neurosci. *12*, 88–104.

Simon, C., Lickert, H., Götz, M., and Dimou, L. (2012). Sox10-iCreERT2: a mouse line to inducibly trace the neural crest and oligodendrocyte lineage. Genesis *50*, 506–515.

Sirko, S., Behrendt, G., Johansson, P.A., Tripathi, P., Costa, M., Bek, S., Heinrich, C., Tiedt, S., Colak, D., Dichgans, M., et al. (2013). Reactive glia in the injured brain acquire stem cell properties in response to sonic hedgehog glia. Cell Stem Cell *12*, 426–439.

Su, Z., Niu, W., Liu, M.L., Zou, Y., and Zhang, C.L. (2014). In vivo conversion of astrocytes to neurons in the injured adult spinal cord. Nat. Commun. *5*, 3338.

Torper, O., Pfisterer, U., Wolf, D.A., Pereira, M., Lau, S., Jakobsson, J., Bjorklund, A., Grealish, S., and Parmar, M. (2013). Generation of induced neurons via direct conversion in vivo. Proc. Natl. Acad. Sci. USA *110*, 7038–7043.

Vierbuchen, T., Ostermeier, A., Pang, Z.P., Kokubu, Y., Sudhof, T.C., and Wernig, M. (2010). Direct conversion of fibroblasts to functional neurons by defined factors. Nature *463*, 1035–1041.